

Helping the Color Blind See Color

Carolyn Chen
Princeton University
Princeton, NJ
clc4@princeton.edu

Dorothy Chen
Princeton University
Princeton, NJ
dschen@princeton.edu

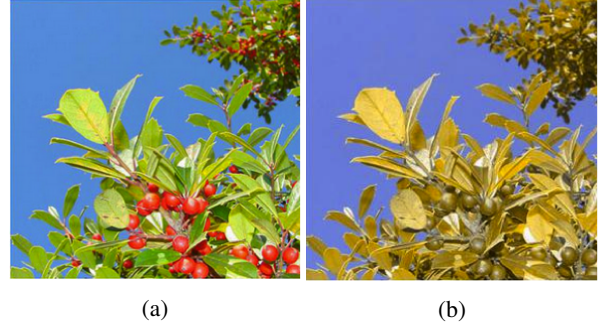
Abstract

In this paper, we discuss a novel way to combine existing research in computer-assisted vision specific to colorblindness in order to generate re-colored images, enhancing accessibility specific to the user. We begin by calibrating the user to detect his or her color vision deficiency (CVD). Following this, we re-color the image based on the user's specific CVD condition. Finally, we assess our results by comparing CVD simulations of the original image and the corrected image.

1. Introduction

Genetic photoreceptor disorders are the most common cause of CVD, manifesting in 8% of Caucasian males, 5% of Asiatic males, and 3% of African-American and Native-American males [3]. With this and the female subset being a substantial portion of the population, it is necessary, in our rapidly growing image-based society, to provide an algorithm that can re-color images to make them more accessible to people with CVD. Without such assistive technology, details that are easily seen by people with normal color vision may be completely overlooked by people with CVD due to differences in color perception (see figure 1). Fortunately, there has been some extensive research on color blindness and re-colorization that work towards reducing such differences in perception. While there is clearly no way to eliminate all differences in perception, these methods have been successful in preserving the semantic information of images between people of different color acuity. We therefore aggregate a few existing techniques in our implementation to serve as a proof of concept as well as a new user-specific system by which images are re-colored.

Normal color vision eyes contain three fundamental photoreceptor cells. These cells, also known as cone cells, are concentrated in the retina near the blind spot, where they are able to absorb the most light. Each type of cone cell has a different spectral response, where the peak sensitivity regions lie in the long (L), middle (M), and short (S)



(a) (b)

Figure 1: (a) is with regular vision; (b) is a simulation of a person with CVD's view

wavelengths [1]. A genetic CVD will cause either a defect or an absence in these cells. Dichromatic colorblindness, which we focus our work on, occurs when one of these cells is absent [2]. The different types of dichromats are protanopes, deuteranopes, and tritanopes, where the L, M, and S cones are missing (respectively). This essentially reduces the color gamut of the dichromate into two-dimensions, as shown in figure 2.

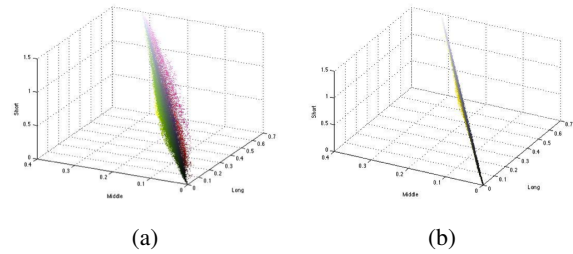


Figure 2: (a) LMS representation with regular vision; (b) LMS under simulation of a deuteranope; Source: use getLMSVisualization.m to visualize an image in LMS space. Note the reduction in space

Because there are three different types of dichromatic conditions, we calibrate the user in the beginning of our color-correction tool through an implementation of a tech-

nique described in [5]. There are several different ways to determine color-blindness, including the widely used Ishihara plates (figure 3). However, a more useful diagnostic test, which is used in [5], is the Farnsworth Dichotomous test, or the D-15 panel test. The D-15 consists of 15 panels of different colors, all chosen to have the same lightness value, that need to be arranged in order in relation to one static panel. This method has proved to be more effective for scientific research because its results can be quantitatively scored, whereas the Ishihara test is simply diagnostic [5]. Because [5] was cited by several papers, we decided to use their method to calibrate our users. Furthermore, not only does it diagnose, but it also provides a way to quantify useful parameters such as the Confusion index, which reveals the severity of colorblindness, and the Selectivity index, which indicates the degree of randomness in the users arrangement. These parameters could potentially be used to make our algorithm even more person-specific.

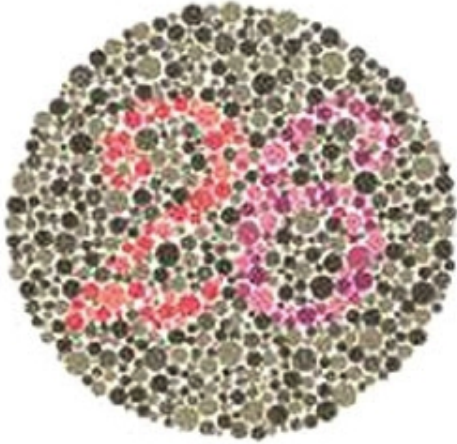


Figure 3: An Ishihara plate, used to diagnose different conditions of CVD

Following this calibration step is the re-colorization algorithm. The goal of this step is to re-color the image based on the users type of CVD so that the user can discern details in the new image that he or she could not do without the enhancement. Authors of [2] propose a re-coloring algorithm that is completely automatic, using a standard four step procedure that involves: 1) finding the key colors of the original image, 2) defining the target distance in the color space to achieve between key colors, 3) an optimization of the mapping of these key colors by minimizing the difference in key color distance between the original and the perceived, and finally 4) re-coloring the image based on the optimization results. The paper claims to exceed previous approaches in both efficiency and effectiveness [2]. It also seemed to have an interesting optimization application, whereas other

methods may naively perform a simple stretch of contrast between the colors of an image, which might consequently create great unnaturalness [4]. Because of these reasons and for the purpose of it being a good learning exercise, we chose to attempt to recreate this algorithm for the project.

We finish our implementation with an algorithm to simulate color-blindness by following the method described in [1], a paper that is widely cited by works related to this topic. This method makes use of the LMS color space to perform the mapping of colors from the original image to the perceived image. Thus, the algorithm consists of mapping the image to LMS space, mapping the physiologically undetermined components, referring to the information marked by the missing cone, to the reduced stimuli surface, and mapping this reduction back to the RGB space. It has been proven to be rather effective in simulating CVD, since people with colorblindness cannot distinguish between the original image and the simulation. We use this algorithm for two purposes: 1) a step in the optimization of the algorithm described in [2] relies on a comparison between a simulation of CVD and the original image, and 2) to serve as a tool for evaluation of this project.

2. Implementation

Here, we discuss in more depth the algorithms that we implemented.

2.1. Calibration

As discussed in Section 1, we used the algorithm described in [5] to quantify the results of the Farnsworth D-15 panel test for colorblindness. Here, we relay a brief description of our user interface, followed by a summary of the algorithm.

The calibration step involves a simple user interface, where the algorithm randomly scatters the different 15 panels at the beginning, thus forcing the user to order the panels relative to the static blue panel on the left (please refer to the readMe file for instructions to execute quickly without this input step). To submit the response, exit out of the window.

The different panels, shown in figure 4, can be mapped to a two-dimensional U^*V^* plane of the 1976 CIELUV color space, since lightness is held constant among them. This makes for a nice and flat mapping of the ordering of the panels (figure 5), where CVDs can be distinguished when orderings cross certain boundaries that distinguish that respective CVDs confusion locus. What the authors of [5] propose is a way to quantify this ordering by using the color difference vectors between the 15 (or 16 including the starting point) caps. They then take these vectors to create relative color difference vectors, as shown in figure 6, where the length of each vector represents the difference in chroma and the angle represents the difference in hue angle (subsequent of the mapping between U^*V^*L and $LCHuv$ space)

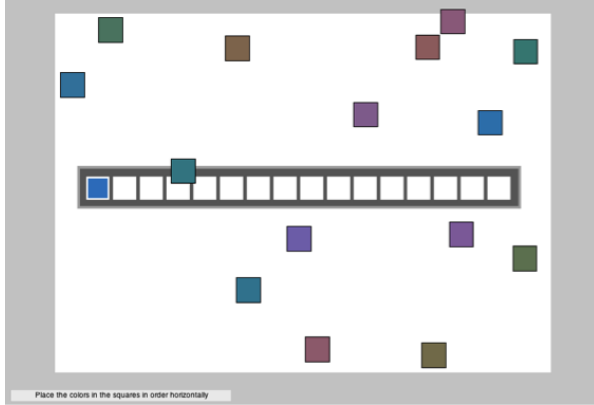


Figure 4: The user interface for calibration

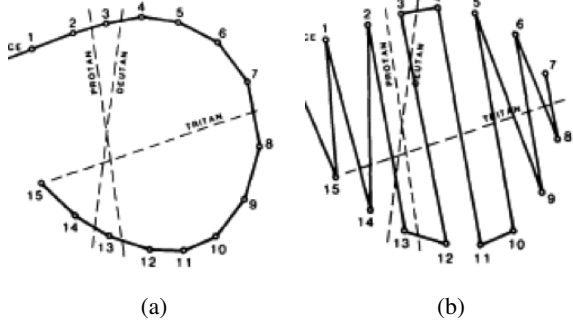


Figure 5: (a) D-15 ordering of panels for normal vision; (b) ordering for a protanope; Source: [5]. the cross-over in the protanope's ordering

of adjacently placed panels.

To analyze this data quantifiably, the authors term their approach the Moment of Inertia Method, where each head of the vector has unit mass and the stem is weightless. The method calls to solve for the principal axes of the system that result in the maximum and minimum moments of inertia of the relative difference vectors. This is done by setting the derivative of the inertia with respect to the axis angle to 0, yielding the equation:

$$\tan(2A) = \sum 2U_n V_n / \sum (U_n^2 - V_n^2) \quad (1)$$

Then, to find the angle of the other axes, it is simply a matter of finding the right angle to A. Finally, to find the corresponding moments of inertia, we plug the angles in the following equation:

$$I = \sum (V_n \cos(A) - U_n \sin(A))^2 \quad (2)$$

The confusion angle, which allows for a quantitative mapping to the type of CVD, corresponds to the angle that yields the minimum moment of inertia. We used comparison statements based off of Table 1 in the paper, which

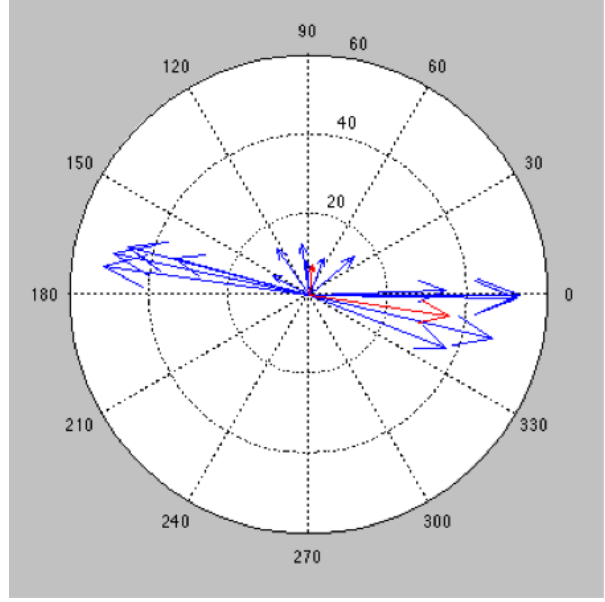


Figure 6: Relative color difference vectors to compute the moment of inertia

contained relevant recommended values for each case of dichromacy, to serve as our diagnosis for the type of CVD. Furthermore, our code calibrate.m returns other useful parameters such as the Confusion index, calculated by dividing the radius of the major axis by the radius of the smaller axis. This indicates the severity of the colorblindness condition, since theoretically a CVD panel arrangement would consist of several crossings, resulting in large vector lengths in very narrow angle ranges. We further calculate the Selectivity index by dividing the major radius by the major radius of a perfect arrangement, which reveals information about the randomness of the arrangement. These extra parameters may serve to be useful to further customize the users experience towards their own unique level of CVD, as we will discuss in section 2.2.d: Gaussian Mapping for Interpolation.

2.2. Re-Colorization

As mentioned in Section 1, we implement the algorithm described in [2]. Here, we summarize the major steps of the algorithm.

2.2.1 Image Representation via Gaussian Mixture Modeling

We first convert the input RGB values to CIE L*a*b* color space, which is capable of describing all colors visible to the human eye and is often used as a device-independent reference. L* refers to the lightness of the color; a* is the position between green and red; and b* is the position be-

tween blue and yellow. A further benefit to representing colors in the L*a*b* color space is that perceptual differences between colors can be approximated by finding the Euclidean distance between points.

We then model the pixels using a Gaussian Mixture Model (GMM), which approximates the distribution of the points as a mixture of K Gaussians. While this can be done using the Matlab function `gmdistribution.fit` [6], we have included the general steps for completeness. Our set of parameters for a mixture of K Gaussians is therefore $\theta_i = (\mu_i, \Sigma_i)$ for each of the K distributions, as well as $\omega_1, \dots, \omega_k$, which are the mixing weights for the Gaussians. As in [2], we shall represent these parameters as Θ . The GMM can be found using the expectation-maximization (EM) algorithm, which is described in [2] as follows:

Expectation step: Given the parameter set Θ^{old} , the probability that pixel x_j belongs to the i^{th} Gaussian is:

$$p(i|x_j, \Theta^{old}) = \frac{\omega_i G_i(x_j|\theta_i)}{\sum_{a=1}^K \omega_a G_a(x_j|\theta_a)}$$

where $G_i(x_j|\theta_i)$ is the probability of x_j given a 3D Gaussian distribution G_i with parameters $\theta_i = (\mu_i, \Sigma_i)$. Therefore, the above expression is the normalized probability that x_j will occur in the i^{th} Gaussian, which is what we are looking for.

Maximization step: This step updates the values for ω_i , μ_i , and Σ_i using the probabilities found in the expectation step. ω_i^{new} is just a re-weighting, where Gaussians with more probable points weighted accordingly; μ_i^{new} is a weighted average for each Gaussian; Σ_i^{new} is a normalized, weighted covariance.

As noted in [2], full covariance matrices are possible. However, using diagonal matrices is a more preferable approach. First, as noted in Matlab documentation online, restricting covariance matrices to diagonal helps prevent ill-conditioned or singular (has no inverse) covariance matrices [6]. Second, this allows for easy inversion of the covariance matrices, which is a necessary step during the calculation of symmetric KL divergence, our way of measuring target distance.

To find the best fitting GMM, we fit several models and choose the one with the smallest Akaike information criterion (AIC), which is measure of both goodness-of-fit and of complexity of a model. As suggested in [2], we generally used values of $2 \leq K \leq 6$. However, we used values of K as large as 12 to see if allowing more complex models would give better results; we decided that the increase in runtime was not worth the increase in performance. See figure 13 for an example.

2.2.2 Target Distance

As mentioned earlier, differences in perception can be approximated in the CIE L*a*b* color space by finding the Euclidean distance between points. Seeing that we have clustered our points using Gaussian distributions, however, the Euclidean distance is no longer a completely informative measure. This is because while we could find the Euclidean distances between means, doing so would ignore the variances of the Gaussians. [2] overcomes this problem by measuring distance using symmetric KL divergence, which is a measure of difference between distributions rather than single points. The symmetric KL divergence can be found as follows:

$$D_{sKL}(G_i, G_j) = (\mu_i - \mu_j)^T (\Sigma_i^{-1} + \Sigma_j^{-1})(\mu_i - \mu_j) + tr(\Sigma_i \Sigma_j^{-1} + \Sigma_j^{-1} \Sigma_i - 2I)$$

where $tr()$ is the trace and I is the 3x3 identity matrix.

2.2.3 Solving the Optimization

We want to find a recoloring of the image such that the contrasts perceived by people with normal vision in the original are the same as the contrasts perceived by people with CVD in the recoloring. In other words, we calculate the symmetric KL divergence for each pair of Gaussians in the original, and we want these values to be as similar as possible to the symmetric KL divergences for each pair of the recolored Gaussians.

To perform the recoloring, we define K mapping functions $M_1(), \dots, M_K()$ for each Gaussian that relocates the mean vector; as in [2], we assume that the covariance matrices are unchanged. We also want to avoid extremely drastic changes in the image, and so we do not change the lightness of the image. In the same vein, we define the mapping functions as rotations in the a*b* plane; this preserves the magnitudes of the colors.

As mentioned earlier, we want to find a mapping such that the symmetric KL divergences of the recolored image are as similar as possible to those of the original. In other words, the error between Gaussians i and j can be found as follows:

$$E_{ij} = [D_{sKL}(G_i, G_j) - D_{sKL}(F_i, F_j)]^2$$

where $F_a = Sim(M_a(G_a))$, or, in other words, the simulated view of the rotated Gaussian. Because some colors are affected by CVD more than others, we weight the errors. To do so, we first find the weights of individual pixels, which is just the Euclidean distance between the original and the simulated images. Recall that this is a good approximation of perceptual differences due to the fact that both images

are in CIE L*a*b* color space:

$$\alpha_j = \|x_j - Sim(x_j)\|$$

We then combine these and normalize to find the weights of the clusters:

$$\lambda_i = \frac{\sum_{j=1}^N \alpha_j p(i|x_j, \Theta)}{\sum_{i=1}^K \sum_{j=1}^N \alpha_j p(i|x_j, \Theta)}$$

where N is the number of pixels in the image.

Therefore, our objective function is a weighted sum of the error terms we found before:

$$\zeta = \sum_{i=1}^K \sum_{j=i+1}^K (\lambda_i + \lambda_j) E_{ij}$$

We minimized this using lsqnonlin and the Levenberg-Marquardt algorithm.

2.2.4 Gaussian Mapping for Interpolation

The CIELAB space, similar to the CIELUV space, can be mapped to cylindrical coordinates corresponding to lightness, chroma, and hue values (LCH). Because the optimized mapping was simply a rotation in the a*b* plane, as described in the previous steps, the L and C value subsequently remain constant while only the hue angle changes. To calculate the new hue value for each pixel, we first find the difference $M(\mu) - \mu$ where M is the mapping rotation, meaning we find the hue shift of each Gaussian cluster. Then, depending on the likelihood of a pixel x_j belonging to the ith Gaussian $p(i|x_j, \theta)$, we calculate the new hue value,

$$T(x_j)^H = x_j^H + \sum_{i=1}^K p(i|x_j, \theta)(M_i(\mu_i)^H - (\mu_i)^H)$$

which takes into account all the shifts and the posterior probability of the pixel. Thus, this accounts for a smooth re-coloring, or interpolation, for the adjusted image.

While the algorithm did not leave room for calibration parameters other than the type of CVD, we hypothesize that there might be a way to incorporate parameters such as severity into the algorithm. For example, for someone who has a deficient amount of L cones as opposed to an absence of all L cones, there will be a response, a reduced response but nevertheless present, of the L cone. Thus, the reduced surface becomes a reduced parallelepiped, and a different mapping can occur. Due to the lack of resources defining this different mapping, we are not able to say with certainty that we have created a re-coloring algorithm that is unique to the user; however, we experimented with a useful parameter returned from calibrate.m, the Confusion Index, which indicates the severity of the CVD.

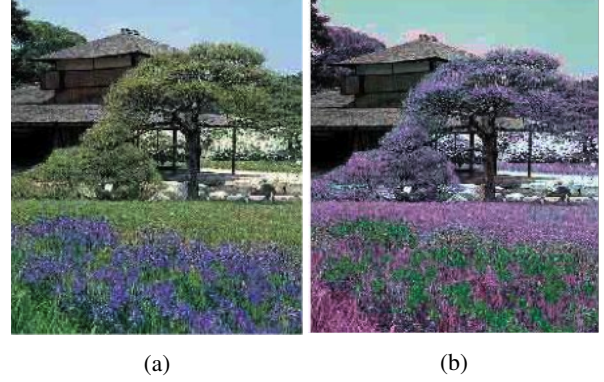


Figure 7: (a) Original image; (b) Re-colored image for a tritanope

Based off of the calibration paper [5], there are approximate values of the C-index that correspond to the different CVD conditions. Thus, in runMe.m, we find the ratio of the retrieved C-index to the known C-index, depending on type. This ratio, upper-capped at one, will determine how we interpolate between the recolored image and the original image: $H(j) = H(j)(1.0 - \text{calib.severity}) + h_j(\text{calib.severity})$ where H is hue and h_j is the recolored hue. *Note, this is not based off of any scientific evidence, as we were unable to access any. The only source that performed an interpolation as well depending on a user parameter was from a Stanford website vischeck that has since closed down. However, we think it is interesting to demonstrate how a user based parameter can affect the outcome, as seen in the following figures.

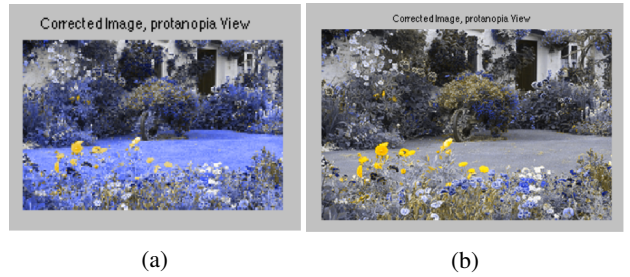


Figure 8: (a) Corrected image for a protanope of severity 1.0; (b) Corrected image for severity 0.5; Note the difference in the brightness of color, where in (a), the contrast between the grass and the yellow flowers is much more accentuated

2.3. Simulation

We implemented the simulation algorithm described in the prevalently cited paper [1]. This can be broken down into three transformation steps, which are described below.

(1) Translate the pixel value to LMS space. This is relatively straightforward, as it is a simple matrix multiplication: $Q = TV$, where Q is the resultant LMS values corresponding to the current pixel, V is the RGB equivalent, and T is composed of the LMS tristimulus values of the Cathode Ray Tube (CRT) monitor used in the paper. The LMS tristimulus values, or the values of the three primaries at maximum intensity, are dependent on the monitor. However, since we did not have access to a spectroradiometer, we were unable to calculate our own LMS tristimulus values corresponding to our personal computers. Thus, we made the assumption that the difference in values between the example that is given in the paper, the Hitachi Model CM2086A3SG Monitor, and our own is minimal and used those values to compose our T and consequently T^{-1} matrix:

$$T = \begin{vmatrix} 0.1992 & 0.4112 & 0.0742 \\ 0.0353 & 0.2226 & 0.0574 \\ 0.0185 & 0.1231 & 1.3550 \end{vmatrix}.$$

(2) Apply the simulation algorithm. Because we are given the maximum limits of the RGB channels in LMS space, we can define a parallelepiped in LMS space that defines all the colors that can be produced by the specific monitor (see figure 9 for a nice illustration). Within this space, depending on the type of colorblindness, is the parallelogram that defines the reduced stimuli surface, since, as we recall, dichromacy occurs when one of the LMS cones is lacking. To map a normal pixel to a simulated pixel, the algorithm projects that value to its corresponding position on the reduced stimuli surface.

Depending on the position of the current pixel with respect to the neutral axis OE , as seen in figure 9, which divides the reduced stimuli surface into two parts, the monochromatic anchor stimulus, in nanometers, is one of two values. In other words, a certain wavelength corresponding to an invariant hue can be assigned as the anchor value for a reduced color, acting as one of two vectors to define the half-plane the pixel is projected down to. The other vector that defines this plane is E , the brightest possible metamer of the equal energy stimulus on the monitor. Here, we assume, due to lack of knowledge of the monitor, that E is represented as $[1;1;1]$ in RGB, or equivalently White, a metamer for white light from the monitor. These two vectors define the plane, and since the cross-product of the two will be orthogonal to the vector defining the new projected pixel, we can solve a series of equations to obtain the mapping of the simulated pixel, taking into account also the loss of information from one of the LMS dimensions.

(3) Re-map back the LMS values to pixel values in RGB space. This step was simple enough, involving a straightforward transformation using the inverse T matrix. To speed up the simulation algorithm, we factored out a lot of code. This was essential because the optimization portion of the

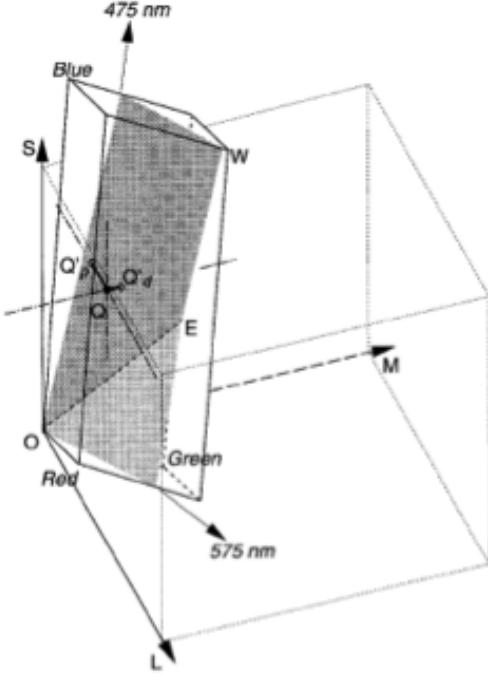


Figure 9: Reduced stimuli surface for a protanope; Source: [1]

algorithm relied on the simulation as well.

3. Results and Evaluation

It was difficult to find a sufficient number of subjects to test our program on to make any significant claims on its success. However, as many of our sources used as well for their evaluation metrics [2-4], we evaluated the “success” of the implementation based on a comparison between the simulated views of the original image and the re-colored image. Through this qualitative sketch, an image would be perceived as a “success” if, between the two simulated images, the re-colored image contained more information regarding color contrast versus the original image.

A possible way to quantify this would be to identify trouble areas that clearly have different colors to a person with normal vision but whose contrast disappears when viewed by a person with CVD. For example, in figure 12, the trouble areas would be the flower and the leaves. We could then convert the image to CIE $L^*a^*b^*$ color space and approximate the perceptual difference between the two areas by finding the Euclidean distance. We can reasonably assume that the difference will be very small when viewing the original image, or else the trouble areas would not be identified as so in the first place. The recoloring would be considered a success if the perceptual difference afterward is greater than some threshold.

Another possible way to evaluate the results, quantifiably, would be to use the Gaussian Mixture Modeling approach used in the re-colorization step to detect key colors in both the simulation of the original and the simulation of the re-colored. If the ratio between the re-colored and the original is greater than 1, then that means that there was a gain in information because there are more key colors. However, when we implemented this metric (`evaluation.m`), we found that the two GMMs always had the same number of clusters: as many as possible. It appears that—at least with the values of K we are working with here—the increased accuracy that results from having more clusters is enough to offset the increased complexity, as both of these criteria are reflected in the AIC (which is used to determine which model is best). Consequently, we could not use this metric to evaluate the performance of our algorithm.

Below are results that demonstrate the “success” of the algorithm introduced by [2]. Here we can clearly see the improvement in the Ishihara plate, where without the color-correction, the number is invisible to the viewer. Testing on natural images, we can see there is an improvement there as well. In the image of the fruit vendor, the simulated original image appears to be selling one long pile of oranges behind the bananas. However, in the re-colored image, the algorithm illuminates the different piles so the viewer can see there are actually three different piles of fruit.

An interesting result from our implementation was the re-colored version of the red flower. As seen in figure 12, re-coloring changed the leaves to blue and the flower to yellow in simulation. Remarkably, the paper that we followed reported a change in, rather, the flower to blue and the leaves to yellow after the re-colorization. It is possible that our implementation of the algorithm gets stuck in a local minimum and is unable to find the global minimum. Because our result essentially just swaps the places of the colors, the symmetric KL divergences will be about equal to those of the paper; this creates a result whose objective function value is extremely close, if not equal, to that of the global minimum.

There are various solutions to this issue, none of which are clearly better than the others. The first is to change the initialization during optimization. While we tried this, we were unable to find one that performed better than what we currently have. The second is to run the optimization multiple times with various initializations, but the increase in runtime may be prohibitive. This is especially true since our colors are essentially the same as the paper’s in this case, just flipped, which means that the increase in performance may not always be substantial. There are other ways to deal with getting stuck in local minima, such as simulated annealing and random restarts, but we didn’t have time to implement these. Again, however, these methods are often extremely costly time-wise.

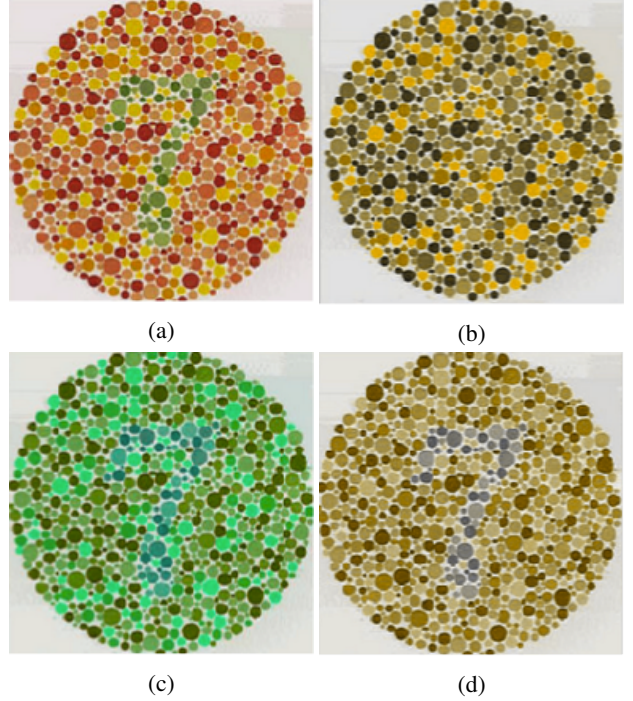


Figure 10: (a) Original image; (b) Original image, protanope view; (c) Corrected image; (d) Corrected image, protanope view, 7 now visible

After implementing the algorithm, we see obvious practical problems with it. For one, it is non-deterministic, as the paper admits that it needs to be performed several times, taking the solution with the least error, to find the best re-colorization. This problem is due to the optimization possibly getting stuck in local minima. As noted above, there are several approaches that we could take to tackle this issue. Furthermore, if there were more time, it would have been interesting to compare the results of another re-colorization algorithm, such as in (Khun), that claims to preserve the naturalness of the image. Here, we see, as in the garden image, that results can sometimes seem very unnatural.

The runtime of the re-colorization step is $O(KN)$ for key color extraction and re-coloring, and $O(K^2)$ for optimization, where K is the number of clusters and N is the number of pixels. Simulation is $O(N)$. This reflects the notable increase in time when a greater number of clusters is considered. For example, one of the largest images in our bank is 312 by 467 pixels in dimension, a little over the biggest image reported by the paper [2]. Our re-coloring implementation takes 23.097 seconds to run for a Gaussian Mixture Model of size 6. For a size of 12, it runs for 111.496 seconds. This runtime is too slow to do real-time processing, although this application would have been useful for other media such as video. Our runtime is about four times slower than the results reported in [2], the reason being that

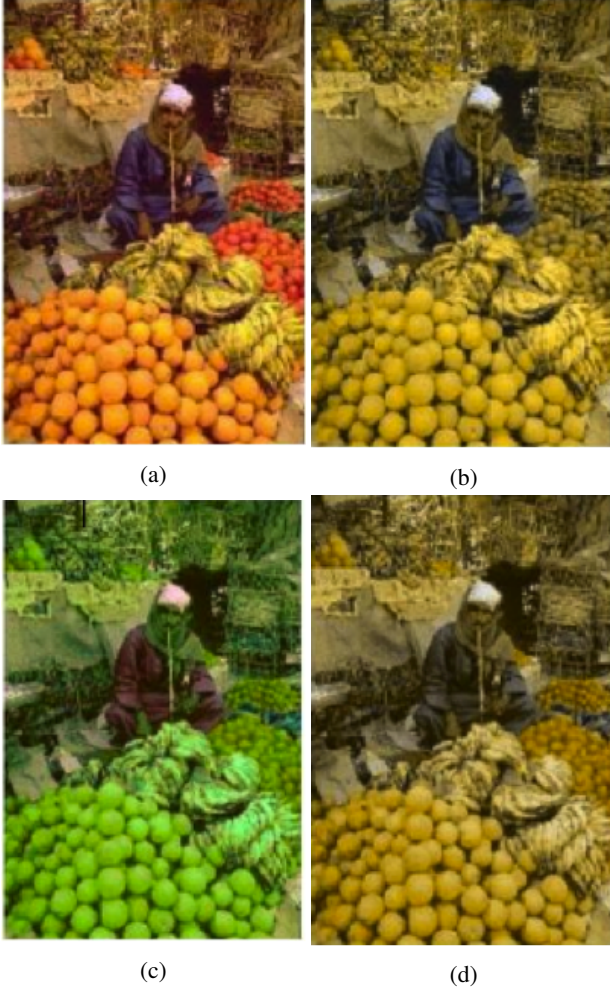


Figure 11: (a) Original image; (b) Original image, deutanope view; (c) Corrected image; (d) Corrected image, protanope view, three piles now visible

we run more iterations in our version to accommodate for occasional non-conversion. We think this is a fair trade-off. The algorithm described in [4] suggests some meddling with the GPU to make computation more efficient, but we did not have enough time to experiment with that.

4. Conclusion

In this paper, we implemented a user-calibrated system to re-color images for people with CVD. We first employed the Farnsworth D-15 panel test to diagnose the user, basing this off of the quantifiable method described in [5]. Then, we followed the algorithm described in [2] to perform the re-colorization of the image. Our evaluation of this method showed that, while it does produce noticeable improvement, it sometimes lacks in naturalness and is not efficient enough to apply to real-time processing. In order to simulate the

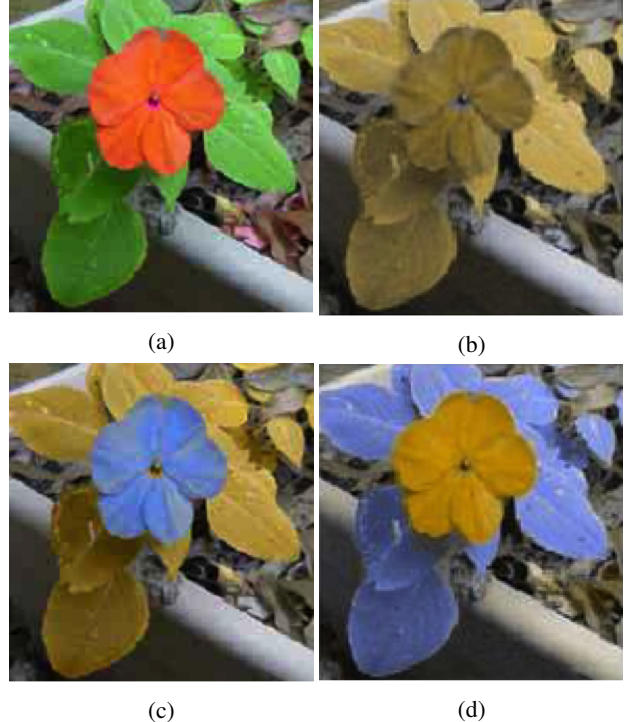


Figure 12: (a) Original image; (b) Original image, deutanope view; (c) Simulated corrected image ([2]); (d) SI simulated corrected image (ours)

differences between the original and re-colored images as viewed by the person with CVD, we implemented the simulation algorithm suggested by [1]. Future work on this topic should be spent towards creating more natural re-colored images as well as searching for a more efficient way to process the images.

5. Acknowledgements

We thank Professor Xiao as well as the TAs of COS 429, Pingmei Xu, Brian Matejek, and Shuran Song. This work has been supported by Princeton University's Department of Computer Science.

6. References

- [1] Brettel, Hans, Franoise Vinot, and John D. Mollon. "Computerized Simulation of Color Appearance for Dichromats." *Journal of the Optical Society of America A* 14.10 (1997): 2647-655.
- [2] Huang, Jia-Bin, Chu-Song Chen, Tzu-Cheng Jen, and Sheng-Jyh Wang. "Image Recolorization for the Colorblind." *IEEE* (2009): 1161-164.
- [3] Jefferson, Luke, and Richard Harvey. "An Interface to Support Color Blind Computer Users." *ACM* (2007).
- [4] Kuhn, Giovane R., Manuel M. Oliveira, and Leandro A. Fernandes. "An Efficient Naturalness-Preserving Image-Recoloring Method for Dichromats." *IEEE* (2008).

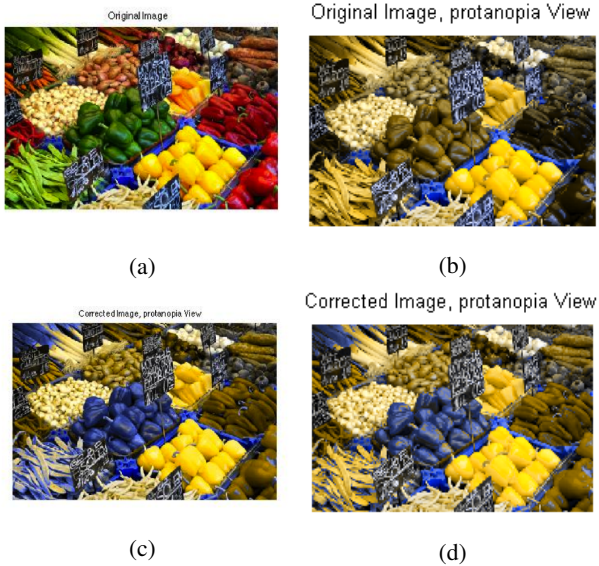


Figure 13: (a) Original image; (b) Simulation of the original image, protanopic; (c) Simulation of corrected image, protanopic, using $K = 6$ when fitting a GMM; note some of the unnaturalness (d) Simulation of corrected image, protanopic, using $K = 12$ when fitting a GMM; note the lessened unnaturalness

[5] Vingrys, Algis J., and P.Ewen King-Smith. "A Quantitative Scoring Technique For Panel Tests of Color Vision." *Investigative Ophthalmology & Visual Science* 29.1 (1988): 50-63.

[6] Matlab documentation for gmdistribution. Retrieved from "<http://www.mathworks.com/help/stats/gmdistribution-class.html>"